



# Adiponectin enhances osteogenic differentiation in human adipose-derived stem cells by activating the APPL1-AMPK signaling pathway



Tong Chen<sup>a, b, 1</sup>, Yu-wei Wu<sup>a, b, 1</sup>, Hui Lu<sup>a, b</sup>, Yuan Guo<sup>a, b</sup>, Zhi-hui Tang<sup>a, b, \*</sup>

<sup>a</sup> Second Dental Center, Peking University School and Hospital of Stomatology, Beijing, China

<sup>b</sup> National Engineering Laboratory for Digital and Material Technology of Stomatology, Peking University School and Hospital of Stomatology, Beijing, China

## ARTICLE INFO

### Article history:

Received 26 March 2015

Available online 17 April 2015

### Keywords:

Adiponectin

Adipose-derived stem cells

Osteogenic differentiation

Bone tissue engineering

APPL1-AMPK signaling

## ABSTRACT

Human adipose-derived stem cells (hASCs) are multipotent progenitor cells with multi-lineage differentiation potential including osteogenesis and adipogenesis. While significant progress has been made in understanding the transcriptional control of hASC fate, little is known about how hASC differentiation is regulated by the autocrine loop. The most abundant adipocytokine secreted by adipocytes, adiponectin (APN) plays a pivotal role in glucose metabolism and energy homeostasis. Growing evidence suggests a positive association between APN and bone formation yet little is known regarding the direct effects of APN on hASC osteogenesis. Therefore, this study was designed to investigate the varied osteogenic effects and regulatory mechanisms of APN in the osteogenic commitment of hASCs. We found that APN enhanced the expression of osteoblast-related genes in hASCs, such as osteocalcin, alkaline phosphatase, and runt-related transcription factor-2 (Runx2, also known as CBFa1), in a dose- and time-dependent manner. This was further confirmed by the higher expression levels of alkaline phosphatase and increased formation of mineralization nodules, along with the absence of inhibition of cell proliferation. Importantly, APN at 1  $\mu\text{g/ml}$  was the optimal concentration, resulting in maximum deposition of calcium nodules, and was significant superior to bone morphogenetic protein 2. Mechanistically, we found for the first time that APN increased nuclear translocation of the leucine zipper motif (APPL)-1 as well as AMP-activated protein kinase (AMPK) phosphorylation, which were reversed by pretreatment with APPL1 siRNA. Our results indicate that APN promotes the osteogenic differentiation of hASCs by activating APPL1-AMPK signaling, suggesting that manipulation of APN is a novel therapeutic target for controlling hASC fate.

© 2015 Elsevier Inc. All rights reserved.

## 1. Introduction

Human adipose derived stem cells (hASCs), ubiquitous within adipose tissue, are multipotent progenitor cells with the capacity for self-renewal and potential for multi-lineage differentiation, including osteogenesis, chondrogenesis, and adipogenesis [1–5]. Since adipose tissue is found throughout the body, is readily available, is plentiful, and has minimal donor site morbidity and immunogenicity, it is an ideal source of cells for the regeneration of

damaged body parts. However, its competence for osteogenic differentiation needs to be enhanced [6–8]. It is known that growth factors, such as bone morphogenetic protein 2 (BMP-2), are effective osteoinductive agents. However, handicaps such as complicated synthesis, easy degradation, and expense restrict its application [9]. Explain adiponectin and osteogenesis here. However, no previously published clinical reports have compared APN with BMP-2 in the osteogenic induction of hASCs.

One of the adipocytokines is APN, a 28-kDa protein that has been reported to influence energy homeostasis, insulin sensitivity, glucose and lipid metabolism, and inflammatory pathways [10,11]. Although recent studies have disclosed that APN influences bone metabolism, many ambiguities remain, as well as conflicting evidence from *in vitro* and *in vivo* studies [12–15]. Moreover, the regulation of the differentiation of stem cells in adipose tissue by adipokines has not been clearly defined.

\* Corresponding author. Second Dental Center, Peking University School and Hospital of Stomatology, B5 Anli Garden, #66 Anli Road, Chao Yang District, Beijing, 100101, China. Fax: +86 10 64907970.

E-mail address: [tang\\_zhihui@live.cn](mailto:tang_zhihui@live.cn) (Z.-h. Tang).

<sup>1</sup> These authors equally contributed.

The current research was commenced to investigate the impact of APN on the proliferation, differentiation, and mineralization of hASCs, with BMP-2 as the positive control. Furthermore, molecular approaches were used to determine how APN directs the destiny of stem cells.

## 2. Materials and methods

### 2.1. Reagents

Human ASCs were from ScienCell Co. (San Diego, CA, USA). Antibodies against APPL1, phospho-AMPK, and AMPK were from Cell Signaling Technology (Beverly, MA). Dulbecco's modified Eagle's medium (DMEM), KnockOut™ Serum Replacement, 100 × penicillin and streptomycin mixture, and 0.125% trypsin-EDTA were from Gibco (NY, USA). The cell counting kit-8 was from Dojindo Laboratories (Kumamoto, Japan). All other reagents were from Sigma–Aldrich (St. Louis, MO, USA) and were all of analytical grade.

### 2.2. Recombinant globular APN (gAPN)

The pEt15b bacterial expression vector encoding the C-terminal of human APN (amino-acids 106–244) was used to express gAPN as a His-tagged protein in BL21 (DE3) bacterial cells. His-tagged gAPN was purified with GE Pharmacia AKTA Purifier 10 (Ramsey, MN, USA) followed by endotoxin removal (L00338, GenScript, Piscataway, NJ, USA) and Zeba Spin Desalting Columns (89893, Pierce, Rockford, IL, USA).

### 2.3. hASC culture and osteogenic induction

hASCs were cultured in fresh DMEM containing 2% (v/v) KnockOut™ Serum Replacement, 100 U/ml penicillin, and 100 mg/ml streptomycin at 37 °C in an incubator with an atmosphere of 95% air, 5% CO<sub>2</sub>, and 100% relative humidity. Cells from the fourth passage were used for all experiments, which were repeated three times using hASCs from three patients. For the cell-differentiation study, the cells were seeded at  $2 \times 10^4$  per well in 12-well plates. After the cultures reached confluence, the medium was changed to DMEM with 2% (v/v) KnockOut™ Serum Replacement, 100 U/ml penicillin, and 100 mg/ml streptomycin containing 10 nM dexamethasone, 10 mM β-glycerophosphate, and 50 μg/ml L-ascorbic acid (Sigma–Aldrich, St. Louis, MO, USA). Then, the cells were further cultured for the indicated times with or without APN, which was synthesized as described previously.

### 2.4. Cell viability assays

The effect of APN on cell viability was evaluated by cell counting kit-8 assay. Briefly, cells were seeded in 96-well plates at  $5 \times 10^4$ /ml and APN was added daily at 0.1, 0.5, 1.0, 5.0, and 10 μg/ml. After 1, 2, 3, 4, 5, 6, and 7 days in culture, the medium was changed and the cells were incubated with the counting reagent for 3 h, according to the manufacturer's instructions. The relative cell number in the cultures was determined by measuring the absorbance of the formazan dye product at 450 nm.

### 2.5. Alizarin red S (AR-S) staining and mineralization assays

hASCs were seeded in 12-well plates at the indicated densities and cultured for 14 or 21 days with osteoinduction. APN was added daily at a concentration of 0.1, 0.5, or 1 μg/ml. Mineralization was determined by staining with 1% (w/v) AR-S in ddH<sub>2</sub>O (pH 4.2) for 1 h at room temperature (RT) on days 14 and 21 of osteoinduction.

After staining, the samples were washed three times with ddH<sub>2</sub>O. To quantify matrix mineralization, AR-S-stained samples were incubated in 100 mM cetylpyridinium chloride for 1 h to solubilize and release calcium-bound AR-S into the solution. The absorbance of the released AR-S was measured at 562 nm.

### 2.6. RNA extraction, reverse transcription, and quantitative real-time PCR

hASCs were seeded in 6-well plates at the indicated densities with or without osteoinduction. APN was added daily at 1 μg/ml. Total cellular RNA was isolated using the TRIzol reagent (Invitrogen, CA, USA). RNA (1.0 μg) was reverse-transcribed into complementary DNA (cDNA) using a PrimeScript 1stStrand cDNA Synthesis kit (TaKaRa, Japan) according to the manufacturer's instructions. Quantification of all gene transcripts was performed with the real-time polymerase chain reaction (qPCR) using Power SYBR Green PCR Master Mix and an ABI PRISM 7500 sequence detection system (Applied Biosystems, Foster City, CA, USA). The gene expression levels were normalized to that of the housekeeping gene GAPDH. The cycle threshold values (Ct values) were used to calculate the fold differences using the ΔΔCt method. The primers used are listed in Table 1 and all primer sequences were determined through established GenBank sequences.

### 2.7. Immunofluorescence

The hASCs were seeded onto coverslips (Φ25 mm) and reached 30–50% confluence before addition of APN. Following APN treatment at the indicated times, cells were fixed in 4% paraformaldehyde for 15 min and then permeabilized in 0.5% Triton X-100 for 5 min at room temperature. After several washes with PBS, the coverslips were blocked in 5% goat serum for 1 h at RT. The primary antibody (1:200) was applied to the coverslips, and incubated overnight at 4 °C. On the next day, the coverslips were washed three times with PBS and incubated in anti-rabbit secondary antibody (1:200, 4412S, Cell Signaling Technology, Beverly, MA, USA) for 1 h at RT. After the nuclei were stained with DAPI, the coverslips were scanned with a Zeiss Axiovert 650 confocal microscope using lasers at 488 nm (green, APPL1) and 405 nm (blue, DAPI). The images were visualized with ImageJ software (NIH, Bethesda, MD).

### 2.8. siRNA-mediated knockdown of APPL1 in hASCs

Several 21-nucleotide small interfering RNA (siRNA) sequences designed to knock down human APPL1 were tested in hASCs. As it is difficult to transfect stem cells, Lipofectamine®2000 Transfection Reagent was used according to the manufacturer's instructions. The hASCs were grown to 30–50% confluence in 6-well plates, and transfected with 100 nM scrambled or APPL1 siRNA for 6 h using Lipofectamine®2000 Transfection Reagent. The siRNA sequence was GCUUAGUUCUUGUCAUGCAtt. APN treatment was commenced 48 h post-transfection and APPL1 knockdown efficiency was assessed by Western blot as described above.

**Table 1**  
Primers used for real time RT-PCR.

Gene	Forward primer (5'–3')	Reverse primer (5'–3')
GAPDH	CAATGACCCCTTCATTGACC	TGGACTCCACGACGTACTCA
RUNX-2	ACTACCAGCCACCGAGACCA	ACTGCTTCGAGCCTTAAATGACTCT
OCN	AGCCACCCGAGACACCATGAGA	AGCCACCCGAGACACCATGAGA
ALP	AACATCAGGGACATTGACGTG	GTATCTCGGTTTGAAGCTCTTCC
OPN	CATACAAGGCCATCCCCGTT	ACGGTGTGCCAATCAGAAG

## 2.9. Western blot analysis

The hASCs grown on 60-mm dishes were harvested with 100  $\mu$ l cell lysis buffer containing phosphatase inhibitor cocktail (Roche, Mannheim, Germany). Cells were scraped from the dish into microfuge tubes. To maximize protein recovery, the cells were also ultrasonicated (Sonics & Materials, Newtown, CT). The protein concentrations in cell lysates were measured with a Pierce BCA protein assay kit (Thermo Scientific, Rockford, US). Protein samples (40  $\mu$ g/lane) in loading buffer were separated by SDS-PAGE gel electrophoresis and transferred onto a polyvinylidenedifluoride membrane (Millipore). After blocking by incubation in non-fat dried milk, the membrane was incubated with the primary antibody (1:1000) overnight. The membrane was then incubated with the secondary antibody marked by IRDye800 and scanned with an Odyssey<sup>®</sup> CLx Infrared Imaging System to visualize the immunoreactive protein bands.

## 2.10. Statistical analysis

Data are expressed as mean  $\pm$  standard deviation. Statistically significant differences ( $P < 0.05$ ) among the various groups were evaluated using one-way ANOVA. All statistical analysis was performed using SPSS 19.0 software (SPSS Inc., Chicago, IL, USA).

## 3. Results

### 3.1. Proliferation of hASCs cultured with APN

The CCK-8 assays showed that APN at 5  $\mu$ g/ml began to slow the cell growth, and proliferation was markedly inhibited when the concentration of APN was  $>5$   $\mu$ g/ml. APN  $\leq 1$   $\mu$ g/ml had negligible effects on proliferation compared with the control group (Fig. 1).

### 3.2. Matrix mineralization of APN-treated hASCs

After 14 days of osteoinduction (OI), the matrix mineralization in the 0.1, 0.5, and 1  $\mu$ g/ml APN groups and the BMP-2 group was superior to that of control. However, only 1  $\mu$ g/ml APN-treated hASCs showed more calcium deposition nodules than the BMP-2 group (Fig. 2). Furthermore, quantitative alizarin red S staining was conducted to study the role of APN in the osteogenic differentiations of hASCs. We noted a substantial augmentation of calcium deposition nodules in the 1  $\mu$ g/ml APN group compared to the other groups. After 21 days of osteoinduction, even more and larger

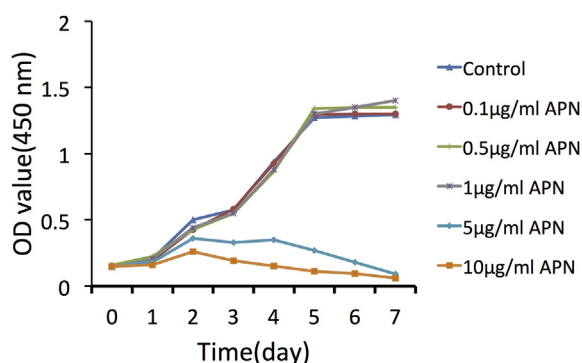


**Fig. 1.** Growth curves for hASCs cultured with different concentrations of APN. There were no significant changes in the proliferative capacity of hASCs cultured with 0.1, 0.5, or 1.0  $\mu$ g/ml APN and hASCs cultured with proliferation medium from days 1–7 ( $P < 0.05$ ). In contrast, APN  $\geq 5$   $\mu$ g/ml had significant adverse effects on the proliferation of hASCs compared with proliferation medium alone.

calcium deposition nodules were observed in the 1  $\mu$ g/ml APN group. Mineralization assays validated the evident superiority of 1  $\mu$ g/ml APN in osteogenic differentiation.

### 3.3. Osteogenesis-related gene expression in APN-treated hASCs

To further confirm the osteogenic capacity of APN, the transcription profile of a panel of osteoblast markers in hASCs cultured with 1  $\mu$ g/ml APN was identified by real-time PCR (Fig. 3). Compared with control, the relative RUNX2, ALP, OCN, and OPN expression rose considerably both with and without osteoinduction. However, compared with the BMP-2 group, the expression of osteogenesis-related genes in 1  $\mu$ g/ml APN group showed an insignificant increase without, but a significant increase with osteoinduction.

### 3.4. Activation of AMPK by APN was APPL1-dependent in hASCs

Having established that APN enhanced the osteogenic differentiation of hASCs in a dose- and time-dependent manner and the concentration of APN for a maximal effect was 1  $\mu$ g/ml, we determined whether AMPK participated in the regulation of osteogenic differentiation. We first assessed whether APN increased the association of APPL1 with the APN receptor (AdipoR) in hASCs. Immunofluorescence imaging of APPL1 disclosed an evidently time-dependent intracellular co-localization in hASCs. APPL1 presented a diffuse cytosolic localization under untreated conditions, while APN treatment for 5 min induced an initial redistribution of APPL1 to the cell membrane, where it was likely to directly bind with AdipoR. However, nuclear and perinuclear localization of APPL1 was observed after 30 min of APN treatment (Fig. 4A). We next used siRNA to knock down the mRNA expression of APPL1. Treatment with targeted siRNA dramatically reduced the APPL1 mRNA expression by 70% according to the qPCR analysis, and achieved 65% APPL1 knockdown as determined by western blot (supplementary data). It was also interesting that the APN-induced stimulation of AMPK phosphorylation was also blunted by the siRNA-mediated reduction of APPL1 levels in hASCs (Fig. 4B). Of note, we found a slight increase in basal AMPK phosphorylation after APPL1 knockdown, with no change in total AMPK expression (Fig. 4C).

## 4. Discussion

There is *in vitro* evidence to show that APN improves the osteogenesis of osteoblastic cell lines such as pre-osteoblast MC3T3-E1 cells [13,15–18]. However, whether APN has the same effects on hASCs was unknown. In order to clarify this, *in vitro* exploration is first needed to determine the optimal concentration threshold and the effectiveness of APN for hASCs. In this study, CCK8 tests showed that APN  $\leq 1$   $\mu$ g/ml did not inhibit cell proliferation, whereas APN  $>1$   $\mu$ g/ml slowed cell growth and markedly inhibited growth when its concentration reached 5  $\mu$ g/ml.

Based on the cell proliferation tests, 0.1–1  $\mu$ g/ml APN was then selected to determine whether APN enhanced the osteogenic differentiation of hASCs and to find the optimal concentration range for osteogenic enhancement. The differentiation of hASCs into osteoblasts was investigated through the assessment of endogenous ALP enzyme activity and extracellular matrix mineralization. When hASCs were treated with 0.1, 0.5, and 1  $\mu$ g/ml APN, more extracellular mineralization occurred in a time- and dose-dependent manner. Because mature osteoblasts are normally characterized by matrix mineralization, we concluded that 0.1–1  $\mu$ g/ml APN enhances the osteogenic differentiation of hASCs *in vitro*, 1  $\mu$ g/ml is the most effective concentration, the osteoinduction by 1  $\mu$ g/ml

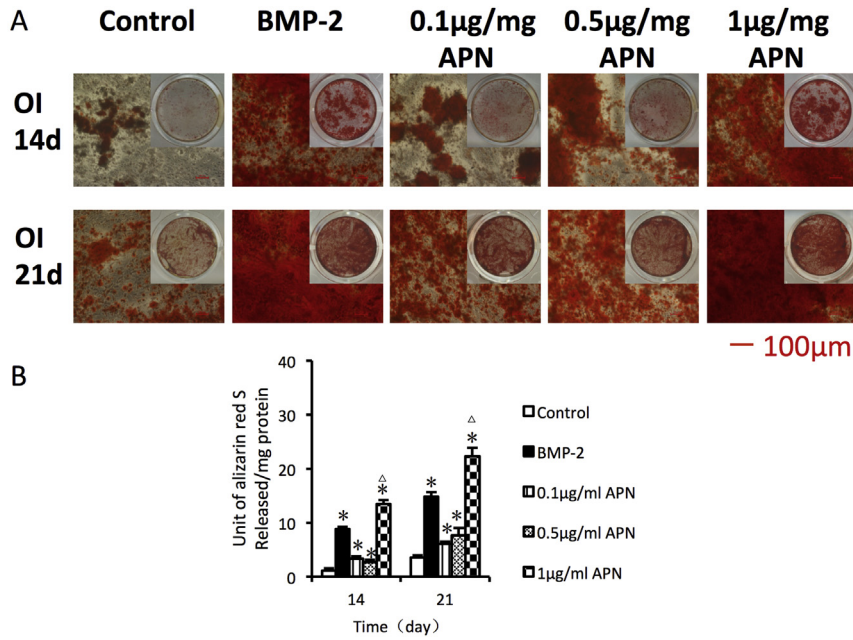


**Fig. 2.** Alizarin Red staining and mineralization assays at days 14 and 21. A: Alizarin Red staining of hASCs at days 14 and 21; B: Quantitative mineralization deposition of hASCs cultured in medium containing different concentrations of APN at days 14 and 21. \*P < 0.05 compared with control group; ΔP < 0.05 compared with BMP-2 group, Cells cultured in osteogenic medium were set as the control group. Scale bars in A, 100 µm. (For interpretation of the references to color in this figure caption, the reader is referred to the web version of this article.)

APN is more prominent in the presence of osteogenic inducers, and is better than BMP-2. because of this, we omitted the lower concentrations in the subsequent experiments. In MC3T3-E1 cells, significant osteogenic enhancement has also been reported for APN at 0.01–1.0 µg/ml [19].

To further explore the signal transduction, we showed, for the first time, that APN mediated APPL1 re-localization in hASCs. APN

stimulated the recruitment of APPL1 to the membrane within 5 min, and this is in keeping with binding to AdipoRs located in the membrane. To determine the functional importance of APPL1 regulation by APN in enhancing osteogenic differentiation of hASCs, we used specific siRNA to knock down APPL1 expression. APN-enhanced osteogenic differentiation was significantly reduced in APPL1-suppressed hASCs compared with scrambled siRNA-

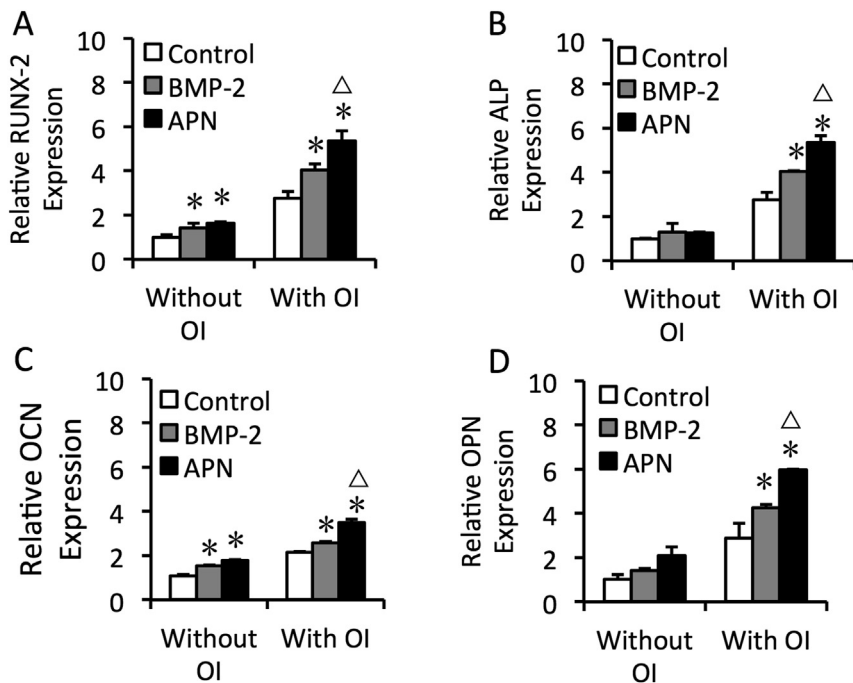


**Fig. 3.** Gene expression profile of osteogenic differentiation-related genes in hASCs cultured with 1.0 µg/ml APN with and without osteogenic induction at day 7 (with Oi and without Oi). A: RUNX-2; B: ALP; C: OCN; D: OPN. \*P < 0.05 compared with control group; ΔP < 0.05 compared with BMP-2 group.

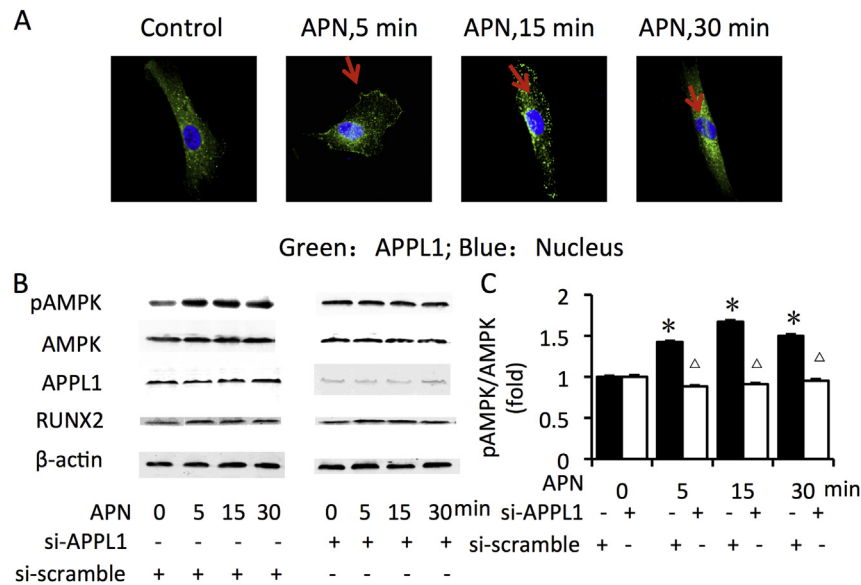


**Fig. 4.** Activation of AMPK by APN was APPL1-dependent. **A:** Immunofluorescence images of APPL1 (green) in hASCs stimulated with APN (1.0 mg/ml) for 5, 15, and 30 min. Cell nuclei were stained with DAPI (blue). Representative images from 3 experiments are shown. Arrows indicate APPL1 re-localization. **B:** hASCs transfected with APPL1 or scrambled siRNA were treated with APN for 5, 15, and 30 min, and immunoblotted for phospho-AMPK, total AMPK, and APPL1 to verify knockdown efficiency. Representative western blots are shown from 3 experiments. **C:** Phospho-AMPK was quantified and normalized to total AMPK. Data represent the mean  $\pm$  SEM from 3 experiments.  $\Delta P < 0.05$  compared with control;  $*P < 0.05$  compared with APN treatment group at corresponding time points. (For interpretation of the references to color in this figure caption, the reader is referred to the web version of this article.)

transfected cells. Adiponectin-mediated RUNX2 expression was also attenuated in hASCs where in which APPL1 had been knocked down. These results indicate that adiponectin enhances osteogenic differentiation of hASCs *via* an APPL1-dependent signaling mechanism.

In the present study, we further explored the underlying molecular mechanisms of the APN-regulated osteogenic differentiation of hASCs. AMPK is a member of a metabolite-sensing protein kinase family that responds to the cellular energy status in eukaryotes. Kim et al. found that the AMPK pathway is activated by an osteogenic medium, and demonstrated that AMPK governs the commitment of hASCs to the osteogenic lineage [20]. Our results showed that APN upregulated the AMPK phosphorylation, suggesting that AMPK is involved in the enhanced osteogenic differentiation. Collectively, these results suggested that APN plays a critical role in enhancing the osteogenic differentiation of hASCs through APPL1-AMPK signaling in the presence of osteogenic inducers.

Many of the effects of APN in various cell types have now been shown to be mediated *via* APPL1, with AMPK as a downstream target [20,21], yet this is the first demonstration of such a mechanism in hASCs. It will be important in future studies to investigate the involvement and functionality of APN and its signaling pathways in regulating hASCs *in vivo*. Other APN signaling targets such as ERK1/2 in the regulation of osteogenic differentiation in hASCs have yet to be studied [22–24].

To sum up, the data we present here first establishes that APN enhances osteogenic differentiation of hASCs *in vitro* by activating the APPL1/AMPK signaling cascade. Our results suggest that APN may serve as a therapeutic agent or target for bone tissue engineering.

#### Conflict of interest

No conflicts of interest, financial or otherwise, were declared by any of the authors.

#### Grants

This work was supported by the National Natural Science Foundation of China (81300851 to Yu-wei Wu), and the Beijing Municipal Natural Science Foundation (SKLODd2009001 to Zhi-hui Tang).

#### Author contributions

Conceived and designed the experiments: ZHT and YWW. Performed the experiments: TC, HL, YG. Analyzed the data: TC, ZHT and YWW. Technical support: RW SHL XFL. Wrote the paper: TC.

#### Appendix A. Supplementary data

Supplementary data related to this article can be found at <http://dx.doi.org/10.1016/j.bbrc.2015.03.168>.

#### Transparency document

Transparency document related to this article can be found online at <http://dx.doi.org/10.1016/j.bbrc.2015.03.168>.

#### References

- [1] B. Levi, M.T. Longaker, Concise review: adipose-derived stromal cells for skeletal regenerative medicine, *Stem Cells* 29 (2011) 576–582.
- [2] X. Li, J. Yao, L. Wu, et al., Osteogenic induction of adipose-derived stromal cells: not a requirement for bone formation *in vivo*, *Artif. Organs* 34 (2010) 46–54.
- [3] J.M. Hong, B.J. Kim, J.H. Shim, et al., Enhancement of bone regeneration through facile surface functionalization of solid freeform fabrication-based three-dimensional scaffolds using mussel adhesive proteins, *Acta Biomater.* 8 (2012) 2578–2586.
- [4] P.A. Zuk, M. Zhu, H. Mizuno, et al., Multilineage cells from human adipose tissue: implications for cell-based therapies, *Tissue Eng.* 7 (2001) 211–228.
- [5] Y. Zhou, Y. Ni, Y. Liu, et al., The role of simvastatin in the osteogenesis of injectable tissue-engineered bone based on human adipose-derived stromal cells and platelet-rich plasma, *Biomaterials* 31 (2010) 5325–5335.

- [6] J.C. Bodle, A.D. Hanson, E.G. Lobo, Adipose-derived stem cells in functional bone tissue engineering: lessons from bone mechanobiology, *Tissue Eng. Part B Rev.* 17 (2011) 195–211.
- [7] W. Tsuji, Adipose-derived stem cells: implications in tissue regeneration, *World J. Stem Cells* 6 (2014) 312.
- [8] M. Ruetze, W. Richter, Adipose-derived stromal cells for osteoarticular repair: trophic function versus stem cell activity, *Expert Rev. Mol. Med.* 16 (2014).
- [9] K. Park, H. Kim, S. Moon, et al., Bone morphogenic protein-2 (BMP-2) loaded nanoparticles mixed with human mesenchymal stem cell in fibrin hydrogel for bone tissue engineering, *J. Biosci. Bioeng.* 108 (2009) 530–537.
- [10] I. Padmalayam, M. Suto, Role of adiponectin in the metabolic syndrome: current perspectives on its modulation as a treatment strategy, *Curr. Pharm. Des.* 19 (2013) 5755–5763.
- [11] T. Villarreal-Molina, C. Posadas-Romero, S. Romero-Hidalgo, et al., The ABCA1 gene R230C variant is associated with decreased risk of premature coronary artery disease: the genetics of atherosclerotic disease (GEA) study., *PLoS One* 7 (2012) e49285.
- [12] I. Kanazawa, Adiponectin in metabolic bone disease, *Curr. Med. Chem.* 19 (2012) 5481–5492.
- [13] K. Oshima, A. Nampei, M. Matsuda, et al., Adiponectin increases bone mass by suppressing osteoclast and activating osteoblast, *Biochem. Biophys. Res. Commun.* 331 (2005) 520–526.
- [14] M. Ruscica, L. Steffani, P. Magni, Adiponectin interactions in bone and cartilage biology and disease, *Vitam. Horm.* 90 (2012) 321–339.
- [15] X.H. Luo, L.J. Guo, L.Q. Yuan, et al., Adiponectin stimulates human osteoblasts proliferation and differentiation via the MAPK signaling pathway, *Exp. Cell. Res.* 309 (2005) 99–109.
- [16] H.W. Lee, S.Y. Kim, A.Y. Kim, et al., Adiponectin stimulates osteoblast differentiation through induction of COX2 in mesenchymal progenitor cells, *Stem Cells* 27 (2009) 2254–2262.
- [17] Y. Mitsui, M. Gotoh, N. Fukushima, et al., Hyperadiponectinemia enhances bone formation in mice, *BMC Musculoskelet. Disord.* 12 (2011) 18.
- [18] D. Fan, L. Li, C. Wang, et al., Adiponectin induces interleukin-6 production and its underlying mechanism in adult rat cardiac fibroblasts, *J. Cell. Physiol.* 226 (2011) 1793–1802.
- [19] I. Kanazawa, T. Yamaguchi, S. Yano, et al., Adiponectin and AMP kinase activator stimulate proliferation, differentiation, and mineralization of osteoblastic MC3T3-E1 cells, *BMC Cell. Biol.* 8 (2007) 51.
- [20] E.K. Kim, S. Lim, J.M. Park, et al., Human mesenchymal stem cell differentiation to the osteogenic or adipogenic lineage is regulated by AMP-activated protein kinase, *J. Cell. Physiol.* 227 (2012) 1680–1687.
- [21] K.K.Y. Cheng, K.S.L. Lam, B. Wang, et al., Signaling mechanisms underlying the insulin-sensitizing effects of adiponectin, *Best. Pract. Res. Clin. En.* 28 (2014) 3–13.
- [22] T. Otani, A. Mizokami, Y. Hayashi, et al., Signaling pathway for adiponectin expression in adipocytes by osteocalcin, *Cell. Signal* 27 (2015) 532–544.
- [23] L. Zhang, K. Wen, X. Han, et al., Adiponectin mediates antiproliferative and apoptotic responses in endometrial carcinoma by the AdipoRs/AMPK pathway, *Gynecol. Oncol.* S0090-8258 (2015) 00652–00656.
- [24] E. Chang, J.M. Choi, W.J. Kim, et al., Restoration of adiponectin expression via the ERK pathway in TNF $\alpha$ -treated 3T3-L1 adipocytes, *Mol. Med. Rep.* 10 (2014) 905–910.